

Observation of Kossel and Kikuchi Lines in Thermal Neutron Incoherent Scattering

B. Sur,¹ R. B. Rogge,² R. P. Hammond,³ V. N. P. Anghel,¹ and J. Katsaras²

¹Atomic Energy of Canada Limited, Chalk River Laboratories, Chalk River, Ontario, K0J 1J0, Canada

²National Research Council, Steacie Institute for Molecular Sciences, Chalk River Laboratories, Chalk River, Ontario, K0J 1J0, Canada

³McMaster University, Department of Physics and Astronomy, Chalk River, Ontario, K0J 1J0, Canada
(Received 9 October 2001; published 25 January 2002)

In this Letter we report the observation of *K* lines (representing collectively, Kossel and Kikuchi lines) produced by monochromatic thermal neutrons interacting with a KDP (potassium dihydrogen phosphate) single crystal. Since *K* lines contain phase information, these observations establish the experimental basis for direct crystallographic phasing of atomic structures containing incoherent scatterers, such as hydrogen, via thermal neutron “inside source” holography.

DOI: 10.1103/PhysRevLett.88.065505

PACS numbers: 61.12.Ex, 89.20.-a

The interaction of single-frequency plane waves with a periodic potential, formulated in the Born approximation, produces diffraction intensities in discrete directions commonly known as Bragg reflections. Similarly, single-frequency spherical waves interacting with a three-dimensional periodic potential (e.g., an atomic lattice) give rise to sharp conical intensity variations. Viewed on a surface, the conic sections appear as lines.

Nearly spherical single-frequency electromagnetic waves are obtained by electronic deexcitations of atoms (e.g., fluorescence, photoemission) within the crystal sample itself, an “inside source,” or in close proximity to the sample. In 1922 Clark and Duane [1] predicted the resulting line structure for x rays and the lines were observed experimentally using a single crystal of copper in 1934 by Kossel, Loeck, and Voges [2]. For x rays, such lines are therefore commonly referred to as Kossel lines. A theoretical explanation was provided in 1935 by von Laue [3]. Spherical waves can also be generated by dynamical effects (e.g., multiple and inelastic scattering) and the resulting lines were first observed by Kikuchi in electron scattering studies using mica plates of varying thicknesses [4]: consequently, such lines are generally referred to as Kikuchi lines. In the present case, thermal neutron spherical waves are generated by incoherent elastic scattering from hydrogen. The fundamental scattering process which gives rise to the characteristic lines—spherical wave interaction with the crystal lattice—is the same as for Kossel and Kikuchi lines, therefore they are collectively referred to as *K* lines.

The *K*-line intensity pattern depends on the relative position of the periodic scatterers with respect to the spherical wave source, i.e., the crystallographic phase of the scattering structure function. Thus *K* lines provide the signal for direct three-dimensional, atomic resolution imaging techniques (holography) for single crystals via the so-called “inside source” [5] or “inside detector” concept [6].

Thermal neutron *K* lines have been predicted theoretically, both for dynamical scattering [7], and due to incoherent elastic scattering [8]. Despite these predictions and to

the best of our knowledge, they have never been identified in experimental thermal neutron scattering data. Town, Smith, and Elcombe [9] carried out a series of constant-**Q** phonon scans, in a lead sample, across the predicted locations for Kikuchi lines and observed a reduction in integrated phonon intensity which they attributed to the neutron Kikuchi effect. Town *et al.* speculated that the direct observation of neutron Kikuchi lines would be difficult, if not impossible [9].

Atomic nuclei are, to a very good approximation, point or pure *s*-wave scatterers of thermal neutron waves. Hydrogen atoms have a large bound, spin-incoherent cross section, $\sigma_i = 80$ barns, for unpolarized thermal neutrons. An unpolarized, parallel, thermal neutron beam interacting with a single crystal containing hydrogen atoms should therefore give rise to both Bragg reflections, from the incident plane-wave neutron beam, and *K* lines, from the spherical waves produced by the incoherent scattering from the H atoms. This experimental approach of using incoherent elastic scattering to obtain *K* lines is different from previous methods using electrons, x rays, and a previous attempt with thermal neutrons [2,4,9–12].

In this Letter data obtained with a monochromatic thermal neutron beam interacting with a KDP (potassium dihydrogen phosphate) single crystal presents strong experimental evidence for thermal neutron *K* lines. Furthermore, the appearance of *K* lines demonstrates that the “holographic oscillations” are not as weak as previously thought [13], and can be extracted from the raw data. Therefore, atomic structure holography using thermal neutrons is possible as was recently demonstrated [14].

To gain an understanding of the process consider a single point spherical wave source of amplitude *a* at the origin, surrounded by a distribution of weak point, or purely spherical wave scatterers described by a coherent scattering length density *b*(**r**). Then, in the Born approximation, the unperturbed or reference wave is

$$\Psi_{\text{ref}}(\mathbf{r}) = \frac{ae^{i|\mathbf{k}||\mathbf{r}|}}{|\mathbf{r}|}, \quad (1)$$

and the scattered or object wave is

$$\Psi_{\text{obj}}(\mathbf{r}) = a \int_{\mathbf{r}_0} \frac{b(\mathbf{r}_0) e^{i|\mathbf{k}|(|\mathbf{r}_0|+|\mathbf{r}-\mathbf{r}_0|)}}{|\mathbf{r}_0| |\mathbf{r}-\mathbf{r}_0|} d\mathbf{r}_0. \quad (2)$$

The total wave amplitude, Ψ_{tot} for a detector at \mathbf{R} , is given by $\Psi_{\text{ref}}(\mathbf{R}) + \Psi_{\text{obj}}(\mathbf{R})$. The detected intensity, $I_{1s}(\mathbf{R})$, is then $\Psi_{\text{tot}}^* \Psi_{\text{tot}}$. Using the far field diffraction condition (i.e., $R \gg r$) and defining the outgoing wave vector in the detector direction as $\mathbf{k}_{\text{out}} = k\hat{\mathbf{R}}$, the detected intensity is then given by

$$I_{1s} \cong \frac{a^* a}{R^2} [1 + 2 \text{Re}[\chi(\mathbf{k}_{\text{out}})] + |\chi(\mathbf{k}_{\text{out}})|^2], \quad (3)$$

where the intensity modulation function is

$$\chi(\mathbf{k}_{\text{out}}) = \int_{\mathbf{r}_0} \frac{b(\mathbf{r}_0) e^{i(kr_0 - \mathbf{k}_{\text{out}} \cdot \mathbf{r}_0)}}{r_0} d\mathbf{r}_0. \quad (4)$$

In “inside source” holography, the scattering length distribution $b(\mathbf{r})$ is reconstructed by a Fourier inversion of the observed intensity modulation [14].

In reciprocal space the modulation function (aside from constants) is given by

$$\chi(\mathbf{k}_{\text{out}}) = \int \frac{B(\mathbf{q})}{|\mathbf{q}|^2 - 2\mathbf{k}_{\text{out}} \cdot \mathbf{q}} d\mathbf{q}, \quad (5)$$

where $B(\mathbf{q})$ is a Fourier transform of $b(\mathbf{r})$.

Consider now the specific case of a crystal lattice. The periodic three-dimensional scattering potential is completely specified by the magnitude and phase of the structure function F_{hkl} at discrete points in reciprocal space. The reciprocal lattice points are given by $\boldsymbol{\tau}_{hkl} = h\mathbf{b}_1 + k\mathbf{b}_2 + l\mathbf{b}_3$, where \mathbf{b}_1 , \mathbf{b}_2 , and \mathbf{b}_3 are three reciprocal lattice basis vectors. The integral in Eq. (5) then becomes a sum over all hkl , namely

$$\chi(\mathbf{k}_{\text{out}}) = \sum_{hkl} \frac{F_{hkl}}{|\boldsymbol{\tau}_{hkl}|^2 - 2\mathbf{k}_{\text{out}} \cdot \boldsymbol{\tau}_{hkl}}. \quad (6)$$

For every pair of discrete points $\pm\boldsymbol{\tau}_{hkl}$, located within a sphere of radius $2k$, the zeros in the denominator of Eq. (6) cause the modulation to go to infinity in \mathbf{k}_{out} directions whose locus is a cone with axis along $\pm\boldsymbol{\tau}_{hkl}$ and full opening angle 2θ satisfying the relation $2k \cos\theta = \boldsymbol{\tau}_{hkl}$. Viewed on the surface of a hemisphere of radius k_{out} the intersection of the cones with the hemisphere are K -line rings centered on $\boldsymbol{\tau}_{hkl}$. These K -line rings are readily calculated for any hkl relative to the crystal coordinate system of a known structure. For example, a selection of the K lines expected for the KDP structure in a particular specimen orientation is illustrated in Fig. 1 on the surface of a unit radius hemisphere, specifically $\mathbf{k}_{\text{out}}/|\mathbf{k}_{\text{out}}|$ with $|\mathbf{k}_{\text{out}}| = 4.8 \text{ \AA}^{-1}$. As well, the incident plane wave, \mathbf{k}_{in} , will produce Bragg peaks, which will appear as discrete points on the surface of the hemisphere, when the condition $\mathbf{k}_{\text{out}} - \mathbf{k}_{\text{in}} = \boldsymbol{\tau}_{hkl}$ is satisfied. This is also illustrated in Fig. 1 where the bright white spots indicate where this Bragg scattering could be observed for KDP in this same

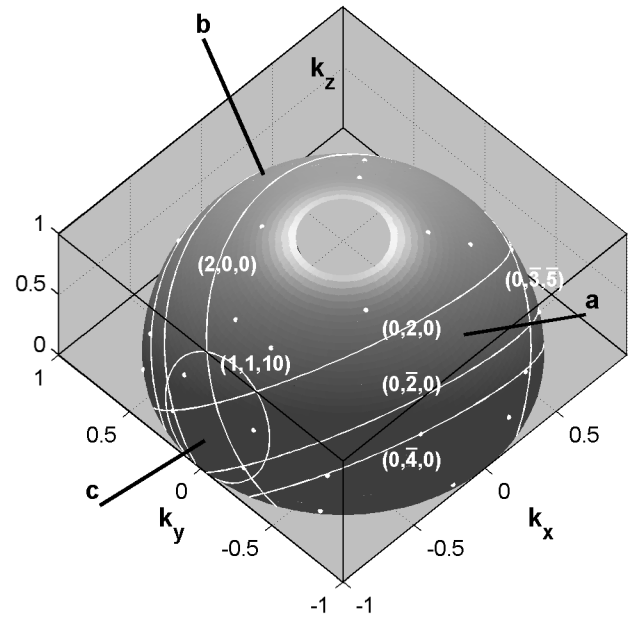


FIG. 1. Calculated K lines for the various lattice planes of the KDP crystal for $\lambda = 1.30 \text{ \AA}$. In addition to the K lines, the location of Bragg reflections, assuming a “thick” Ewald sphere ($|\mathbf{k}_{\text{out}} - \mathbf{k}_{\text{in}}| \pm \Delta k$, where $\Delta k/k = 3\%$), are shown as white spots. The orientation of the crystal with respect to the sphere-of-scattering ($\mathbf{k}_{\text{in}} \parallel k_z$) is depicted by the crystallographic axes a , b , and c .

sample and beam orientation ($\mathbf{k}_{\text{in}} \parallel k_z$). It is therefore expected that these two effects should be observed experimentally by directing a collimated, monochromatic, neutron beam toward a H-containing single crystal (i.e., KDP) and obtaining data over a hemisphere of scattering.

The sample was a rectangular parallelepiped, single crystal of KH_2PO_4 (KDP) of dimensions $1 \times 1 \times 0.5 \text{ cm}^3$ purchased from Cleveland Crystals, Inc. (Highland Hts., OH). The KDP crystal structure is of the tetragonal body-centered space group $I\bar{4}2d$ with unit cell parameters $a = 7.453(1) \text{ \AA}$ and $c = 6.973(1) \text{ \AA}$ [15]. The present data were acquired using the $E3$ triple-axis spectrometer located at the NRU reactor (Chalk River Laboratories). A sketch of the experimental setup is given in Fig. 2. A monochromatic neutron beam of wavelength $\lambda = 1.30 \text{ \AA}$, and estimated wavelength resolution $\Delta\lambda/\lambda \sim 1.5\%$ was obtained from a (113) reflection of a Ge single crystal monochromator. The sample-to-detector angular resolution was limited by distance collimation, as defined by a combination of an aperture and the sample size to 2° vertically and 2° horizontally. The sample orientation (ϕ) and detector angle (θ) were manipulated to optimally tile the scattered wave vector, \mathbf{k}_{out} , over most of a hemisphere ($14^\circ \leq \theta \leq 90^\circ$) of scattering from the sample.

In a high resolution experiment K lines are readily identified by their characteristic fine structure [8,16]. The resolution offered by the present experiment does not permit such identification. K -line fine structure is affected by

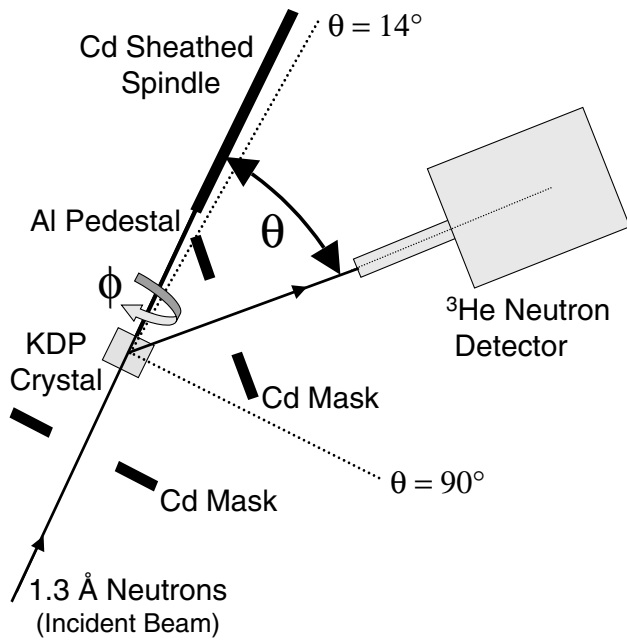


FIG. 2. Schematic view of the experimental setup used to observe K lines from a single crystal of KDP. The (113) planes of a Ge monochromator were used to provide 1.30 \AA neutrons with $\Delta\lambda/\lambda \sim 1.5\%$. The KDP crystal was secured on an aluminum pedestal with thin aluminum wires and which in turn was attached to a long cadmium sheathed spindle. The angle of sample rotation is denoted ϕ while the angle between the detector and the ϕ axis is θ . In order to efficiently obtain the hemisphere of scattering the crystal was rotated, in optimal ϕ steps of $2^\circ/\sin\theta$ from 0 to 2π for a given θ . In the present experiment θ spanned the range from 14° to 90° in 2° steps. The scattered neutrons were detected using a ^3He detector.

numerous factors such as (a) sample size and shape; (b) dynamics or higher order partial wave scattering in both the periodic coherent and incoherent scatterers which lead to broadening of the signal and a nonuniform reference wave intensity; (c) wavelength spread and angular resolution. All of these effects conspire to mute the sharp modulations characteristic of K lines but should still produce modulations along lines as illustrated in Fig. 1.

Figure 3(a) shows the raw intensity data on the surface of a hemisphere of unit radius, containing $5023 \text{ } 2^\circ \times 2^\circ$ solid-angle pixels. The data contain scattering from the KDP sample plus a θ -dependent background due to powder lines from the Al pedestal and Al wires used to mount the sample (see Fig. 2). The measurements were repeated without the sample. This measured background, scaled by the measured sample transmission, was subtracted from the raw intensity data. The remaining scattering intensity distribution $I(\theta, \phi)$ contains a θ -dependent variation dominated by the incoherent elastic scattering Debye-Waller factor for the H atoms. There is also a regular variation in both θ and ϕ , reflecting the sample shape, due to self-attenuation by the sample. The variations were estimated by a least-squares fit of the background subtracted intensity to a phenomenological function of the

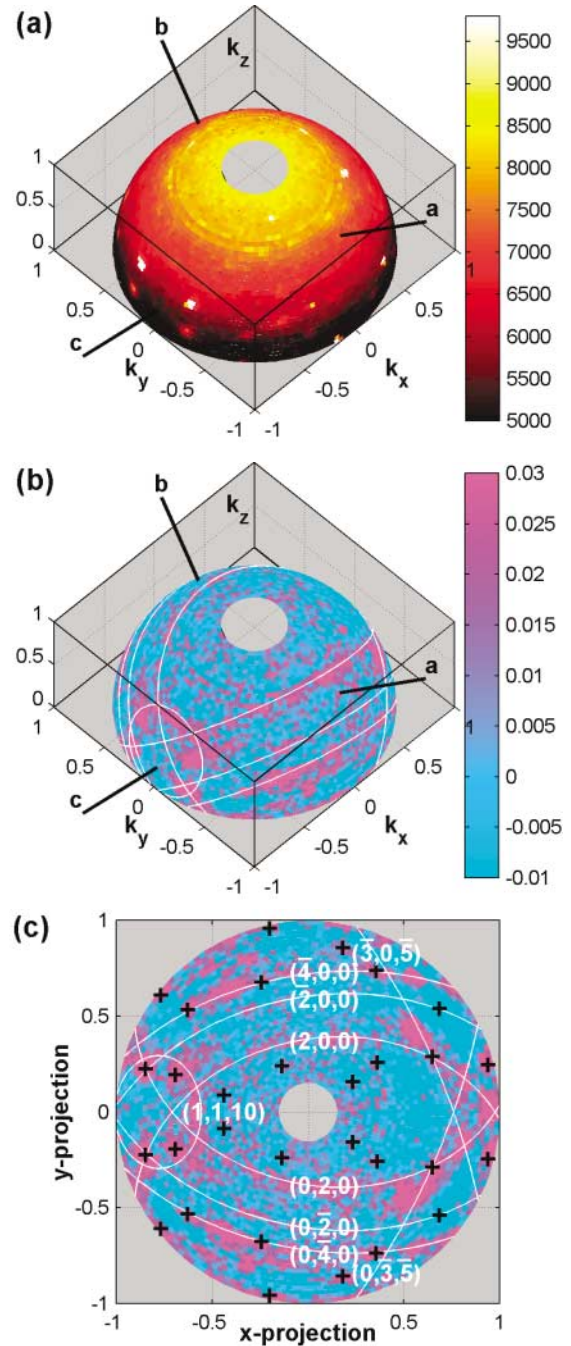


FIG. 3 (color). (a) Raw counts (indicated by color) vs $\hat{\mathbf{k}}_{\text{out}}$ plotted in $2^\circ \times 2^\circ$ pixels with $|\mathbf{k}_{\text{out}}| = 4.8 \text{ \AA}^{-1}$ ($\mathbf{k}_{\text{in}} \parallel k_z$). Bragg spots are clearly visible in the data, but the K -line modulations are too small compared to the dynamic range of the data. (b) Data corrected for background, Debye-Waller factor, and sample shape. Bands of scattering are now clearly visible and follow calculated K lines (white lines) corresponding to those in Fig. 1. (c) The complete corrected data set, shown in a projection [$x = (2\theta/\pi) \cos\phi$, $y = (2\theta/\pi) \sin\phi$]. The calculated K lines and Bragg spots from Fig. 1 are also shown.

form $D(\theta) = \alpha_1 e^{[\alpha_2(1-\cos\theta)]}$ (α_i are fitted parameters) for the Debye-Waller factor and to a shape function, $S(\theta, \phi)$, obtained by finite element modeling (with adjustable

parameters) of the sample attenuation effect. The corrected data given by $C(\mathbf{k}_{\text{out}}[\theta, \phi]) = I(\theta, \phi)/D(\theta)S(\theta, \phi) - 1$ is then proportional to $2\text{Re}[\chi(\mathbf{k}_{\text{out}})] + |\chi(\mathbf{k}_{\text{out}})|^2$.

Figure 3(b) depicts $C(\mathbf{k}_{\text{out}})$ over the same hemisphere as shown in Figs. 1 and 3(a). The orientation of the crystal used for the calculation of the K -line loci in Fig. 1 was chosen to match the known orientation of the KDP crystal for the measurements. Apart from the evident and intense Bragg reflections, the modulation for any given pixel is, at most, 5% above the local diffuse intensity. The entire corrected data set is visible in the projection shown in Fig. 3(c). The calculated K lines and Bragg spots from Fig. 1 are superimposed on this projection. The evident bands of intensity in the corrected scattering data correspond to the calculated K lines. A limited subset of the allowed Bragg reflections will satisfy the conditions necessary to produce a spot on the surface of the scattering hemisphere. However, in order to account for weak scattering from a possible feed-through of Bragg reflections corresponding to reciprocal lattice points that would normally lie outside the Ewald sphere, a “thick” Ewald sphere ($|\mathbf{k}_{\text{out}} - \mathbf{k}_{\text{in}}| \pm \Delta k$ with $\Delta k/k = 3\%$) was used to calculate the positions of Bragg spots indicated in Figs. 1 and 3(c). It can be seen that some of the predicted Bragg spots coincide with some locations of intense scattering. More importantly, however, it is also clear that the bands of scattered intensity, which coincide with the expected K lines (Fig. 1), are not just a chance coalescing of Bragg scattering.

In 1983, Wilkins proposed the observation of K lines using neutrons that had undergone inelastic diffuse scattering from phonons [7]. An experiment relevant to the theory by Wilkins was carried out by Town, Smith, and Elcombe [9]. Their experimental results were consistent with the neutron Kikuchi effect. However, they speculated that direct observation of neutron K lines would require an intense source and very good angular resolution, making the observation of K lines with neutrons difficult, if not impossible.

We have shown that neutron K lines are directly observable using incoherent elastic neutron scattering, as pre-

dicted by Petrascheck [8]. The present result provides direct evidence for a fundamental diffraction phenomenon of neutron spherical waves interacting with a three-dimensional periodic potential. These experimental results open the door for applications of thermal neutron K lines, particularly the direct determination of crystallographic phases in hydrogen-rich materials. These data also clarify the nature of the hologram modulation signal for single crystals, and confirm that atomic structure thermal neutron holography is viable as was demonstrated recently [14].

-
- [1] G. L. Clark and W. Duane, Proc. Natl. Acad. Sci. U.S.A. **8**, 90 (1922).
 - [2] W. Kossel, V. Loeck, and H. Voges, Z. Phys. **94**, 139 (1935).
 - [3] M. v. Laue, Ann. Phys. (Leipzig) **23**, 705 (1935).
 - [4] S. Kikuchi, Jpn. J. Phys. **5**, 83 (1928).
 - [5] A. Szöke, in *Short Wavelength Coherent Radiation: Generation and Applications*, edited by T. Attwood and J. Boker, AIP Conf. Proc. No. 147 (AIP, New York, 1986); A. Szöke, Phys. Rev. B **47**, 14044 (1993).
 - [6] T. Gog, P. M. Len, G. Materlik, D. Bahr, C. S. Fadley, and C. Sanchez-Hanke, Phys. Rev. Lett. **76**, 3132 (1996).
 - [7] S. W. Wilkins, Phys. Rev. Lett. **50**, 1862 (1983).
 - [8] D. Petrascheck, Phys. Rev. B **31**, 4043 (1985).
 - [9] S. L. Town, T. F. Smith, and M. M. Elcombe, Aust. J. Phys. **42**, 289 (1989).
 - [10] Z.-L. Han, S. Hardcastle, G. R. Harp, H. Li, X.-D. Wang, J. Zhang, and B. P. Tonner, Surf. Sci. **258**, 313 (1991).
 - [11] S. Marchesini, M. Belakhovsky, A. Q. R. Baron, G. Faigel, M. Tegze, and P. Kamp, Solid State Commun. **105**, 685 (1998).
 - [12] J. T. Hutton, G. T. Trammell, and J. P. Hannon, Phys. Rev. B **31**, 743 (1985).
 - [13] G. Faigel and M. Tegze, Rep. Prog. Phys. **62**, 355 (1999).
 - [14] B. Sur, R. B. Rogge, R. P. Hammond, V. N. P. Anghel, and J. Katsaras, Nature (London) **414**, 525 (2001).
 - [15] J. E. Tibbals, R. J. Nelves, and G. J. McIntyre, J. Phys. C **15**, 37 (1982).
 - [16] T. Gog, D. Bahr, and G. Materlik, Phys. Rev. B **51**, 6761 (1995).